An Investigation on the Data Mining to Develop Smart Tire

Jae-Cheon Lee[1], Hao Liu[1], Young Gi Seo[2], Seong Woo Kwak[2], Ho Seung Lee[1], Hae Jun Jo[1] and
Sangsu Park[2]

[1]*Department of Mechanical and Automotive Engineering, Keimyung University, 1095 Dalgubeol-daero, Daegu, S. Korea*
[2]*Department of Electronic and Electrical Engineering, Keimyung University, 1095 Dalgubeol-daero, Daegu, S. Korea*

Keywords: Data Mining, Smart Tire, Tire Built-in Sensor, Strain Gage, Tire Deformation Value, Vehicle Load.

Abstract: A smart tire is required to improve driving safety for an intelligent vehicle especially for automated driving electric vehicles. It is necessary to provide information of tire contact forces (vertical, longitudinal, and lateral directions) to control velocity and steering angle of the autonomous vehicle so as to ensure driving stability. This study presents a smart tire system with the data mining to estimate the vertical load by using the tire deformation data in particular. Firstly, the hardware system construction of the smart tire in which tire deformation on driving by using strain gauge is described. And then the test condition is set up and total 27 sets of experimental data are processed to perform correlation analysis for specifications of measured waves. Next, the estimation algorithm of smart tire vertical load is derived by considering the area of tire-ground contact patch and also by introducing compensate coefficient of transverse direction length of contact area. The experimental results show the proposed estimation algorithm is feasible and precise. The advanced adaptive and precise estimation algorithm with artificial neural network will be developed further.

1 INTRODUCTION

As the fourth industrial revolution approaches, the development of automated driving vehicles has been undertaken by major car manufactures with supplier companies and various research institutes. While electric powered complete autonomous car is final goal, its safety and reliability issues must be solved for commercialization.

Conventional vehicle motion control systems estimate the grip force between the tire and the road as well as the coefficient of road friction, the rigidity and the slip angle based on the mathematical vehicle dynamics model. However, the dynamic power transfer rate from the power pack to the wheels of an electric car is over 10ms faster than that of the internal combustion engine's vehicle. And the driving safety of automated driving cars need immediate response on the current road-vehicle situation. Therefore, in order to reduce the time to calculate the grip force between the tire and the road, sensors must be built into the tire and be directly measured in real time. As such, tires built-in sensors are referred to smart tires (Park and Gerdes, 2015).

Measurement of the real-time deformation of a tire has been a challenge in the field of smart tire

development (Matsuzaki and Todoroki, 2008). This study used strain gauge sensor incorporated inside the tire to measure the deformation of a tire. Then, a unique algorithm was proposed to estimate the vehicle load on each tire based on the time-varying deformation data obtained by data mining technique in real time. A method was also developed to accurately calculate the ground area with the road surface. To verify the proposed algorithm, a sensor-driven electrical circuit was designed and a load measurement experiment was conducted using the vehicle tester. In addition, the measurement system was implemented to detect the deformation of the tire in real time.

The composition of this paper is as follows: Section 2 describes the real-time instrumentation system for detecting the deformation of a tire, and the experimental conditions and data analysis are given in Section 3. Section 4 proposes an algorithm to obtain the vertical load using the measured deformation data. It also describes how the parameters needed for the proposed algorithm are extracted. Section 4 shows the accuracy of proposed algorithm by comparing the experimental actual load and estimated load. Finally, Section 5 draws conclusion.

2 SMART TIRE SYSTEM

Strain gauge sensor is a sensor that measures load by using the properties that change resistance depending on the force applied. The compression and length variation of the strain gauge results in a change in resistance, which is indicated by a change in voltage (Ahn, Bae and Kim, 2003). This study has used a strain gauge with a wire length of 150mm and a resistance of 120Ω. NI 9237 module with built-in Wheatstone Bridge circuit was also used to measure the output voltage signal of the strain gauge. Figure 1 and Figure 2 show the schematic and photos of the smart tire instrumentation system composed by the strain gauge, NI 9237 module and a slip-ring respectively.
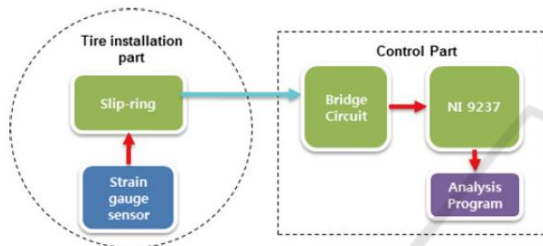

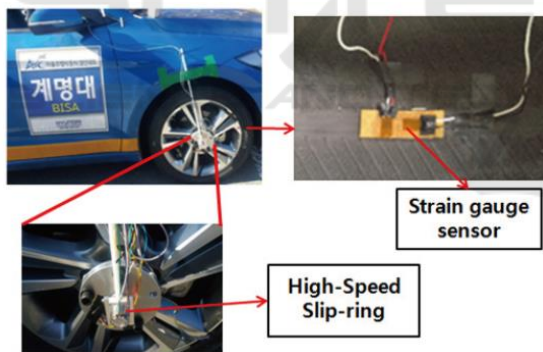Figure 1: Schematic of a smart tire system.

Figure 2: Strain gauge sensor and slip-ring mounted on a tire and wheel.

3 EXPERIMENT AND DATA PROCESSING

3.1 Experiment Description

After the acquisition system using the strain gauge is constructed test experiment should be design. Only vertical load acting on the tire is firstly considered. It is well known that there are lots of factors which can effect tire deformation in vertical direction.

Therefore, the objective of test experiment is to collect information which contains relation between tire deformation reflected by the strain gauge and these factors.

Three main factors, i.e. tire vertical load, tire air charging pressure, and tire center speed (vehicle speed), are considered in the test experiment. They are set as following values:

- *Vertical load*: 285kgf, 300kgf, 315kgf. The total weight of the test vehicle is about 1.2Ton and the vertical load acting on each tire is 300kgf with ± 5% variations (±15kgf);
- *Pressure*: 33psi, 35psi, 37psi. The standard tire air charging pressure is 35 psi and variation with ± 2psi is set;
- *Speed*: 25kph, 30kph, 35kph. Low speed is tested at first to ensure experiment success.

As a result, there are 27 different experimental conditions totally. In order to keep tire constant speed all experiments were performed on a tire test rig.

3.2 Data Processing and Specification Extraction

The raw signal (red dotted line) measured by the strain gauge is shown in Figure 3, which obviously contains lots of noise. Noise contained in the original strain gauge is mainly eliminated by using a wavelet decomposition at the level 3 with a symlet wavelet. The two waveforms in Figure 3 mean that the tire part where the strain gauge adheres contacts with the ground as the tire rolls while the period between two waveforms imply that the part rolls out from the ground and hasn't other deformation but deformation due to tire pressure. The strain gauge signal during this period shows the normal deformation of the tire. Accordingly, the value of the strain gauge signal during this period is selected as a base line (green dashed line in Figure 3) of the waveform. Because most of measured voltage value distributes around the base line it is easy to determine its value by using histogram distribution. Figure 3 shows the measured strain gauge signal with the vertical load of 285kgf, the speed of 25kph, and the pressure of 33psi.

In order to extract features of the strain gauge waveform the following five specifications are defined as shown in Figure 4.
- *Base line value*: the distance between the base line and the zero horizontal axis;
- *Max peak value*: the peak value from the base line;
- *Min peak value*: the trough peak value from the base line;
- *Peak duration*: the time length of a waveform;

- *Peak-peak interval*: the time interval between two neighboring waveform peaks.

Base on above definitions the five specifications of all acquired strain gauge signal for one experimental condition can be calculated and then the average value of them is obtained, which is shown in the Table1.

Table 1: Calculated specifications for different experimental conditions.

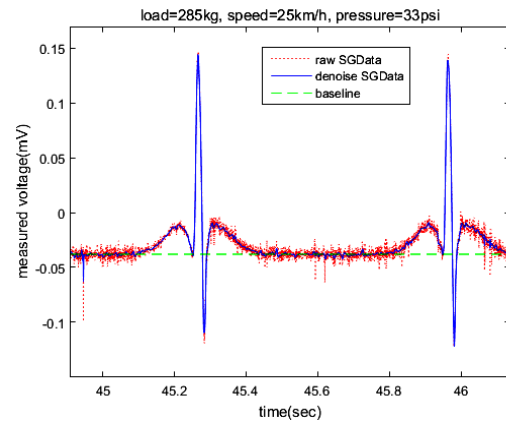| No.	Load (kgf)	Speed (kph)	Pres. (psi)	Base line	Max peak	Min peak	Duration	PP interval
1	285	25	33	-0.038	0.179	0.079	0.038	0.692
2	300	25	33	-0.031	0.163	0.077	0.038	0.688
3	315	25	33	-0.027	0.151	0.074	0.038	0.681
4	285	30	33	-0.035	0.183	0.083	0.032	0.576
5	300	30	33	-0.030	0.170	0.086	0.032	0.573
6	315	30	33	-0.027	0.157	0.080	0.032	0.573
7	285	35	33	-0.033	0.188	0.085	0.028	0.494
8	300	35	33	-0.029	0.175	0.085	0.028	0.494
9	315	35	33	-0.026	0.164	0.080	0.028	0.493
10	285	25	35	-0.061	0.207	0.072	0.047	0.694
11	300	25	35	-0.049	0.199	0.070	0.046	0.694
12	315	25	35	-0.043	0.192	0.070	0.045	0.693
13	285	30	35	-0.054	0.215	0.078	0.040	0.578
14	300	30	35	-0.048	0.212	0.076	0.038	0.578
15	315	30	35	-0.042	0.204	0.077	0.038	0.578
16	285	35	35	-0.051	0.225	0.081	0.034	0.496
17	300	35	35	-0.045	0.221	0.081	0.032	0.494
18	315	35	35	-0.040	0.209	0.079	0.031	0.492
19	285	25	37	-0.108	0.312	0.104	0.049	0.695
20	300	25	37	-0.086	0.241	0.079	0.050	0.692
21	315	25	37	-0.072	0.224	0.071	0.049	0.695
22	285	30	37	-0.094	0.276	0.092	0.041	0.579
23	300	30	37	-0.078	0.242	0.080	0.042	0.579
24	315	30	37	-0.066	0.232	0.082	0.042	0.579
25	285	35	37	-0.086	0.274	0.090	0.038	0.497
26	300	35	37	-0.074	0.251	0.081	0.037	0.496
27	315	35	37	-0.062	0.240	0.084	0.036	0.496

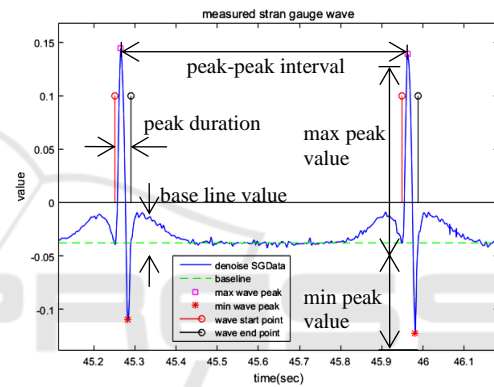Figure 3: Filtered strain gauge wave by using wavelet transform.

Figure 4: Definitions of specifications of the measured strain gauge wave.

3.3 Specification Analysis

In order to investigate how the three factors (the vertical load, the tire air pressure, and the speed) effect the five specifications the calculated specifications are represented in Figure 5 to Figure 9. Two horizontal axes are the vertical load and the pressure, respectively, in these figures and the vertical axis represents variation of specifications with three different speeds.

The following conclusions can be drawn from each figure:

- Base line value: shows the normal state when the local part of the tire does not contact with the ground. The higher the tire air pressure is, the further the base line deviates from zero, which means tire deformation is more serious.
- Max peak value: increases with increasing of pressure and decreasing of vertical load. The higher air pressure leads to the greater deformation of the tire. The higher speed causes

the greater peak value, however it is inverse in high pressure and low vertical force.

- Min peak value: indicates almost same trend as the max peak value.
- Peak duration: obviously increases with decreasing of speed. Meanwhile it rises up in high tire pressure but is not sensitive to the vertical load.
- Peak-peak interval: shows the same behaviors with the speed as peak duration. And it keeps almost constant value regardless of the vertical load and the pressure.
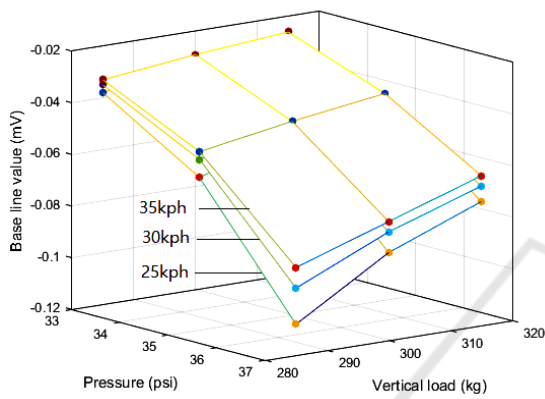

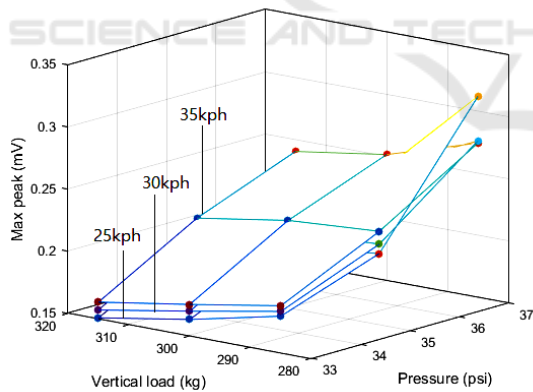Figure 5: Base line variation VS. vertical load, pressure, and speed.

Figure 6: Max peak variation VS. vertical load, pressure, and speed.
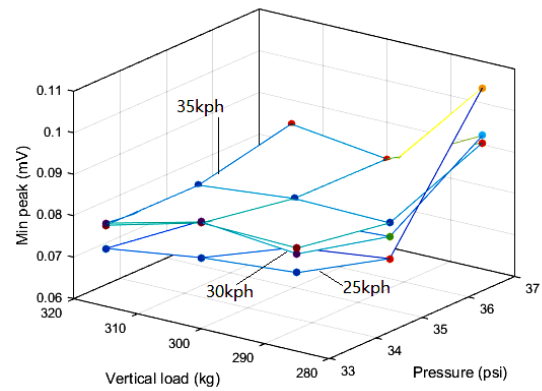

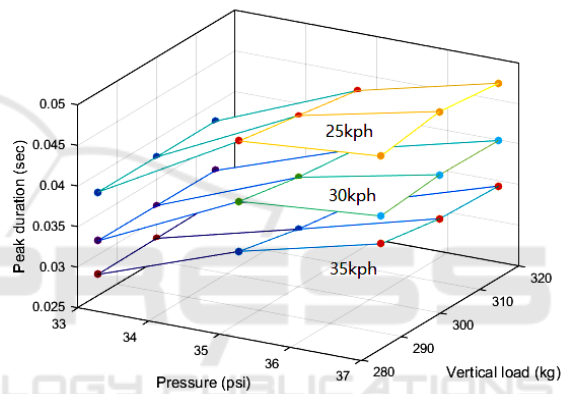Figure 7: Min peak variation VS. vertical load, pressure, and speed.

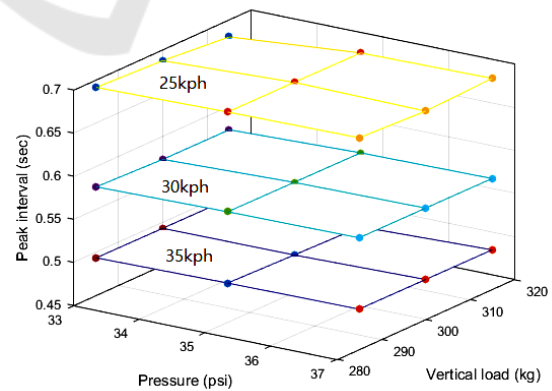Figure 8: Peak duration variation VS. vertical load, pressure, and speed.

Figure 9: Peak-Peak interval variation VS. vertical load, pressure, and speed.

4 LOAD ESTIMATION ALGORITHM

4.1 Tire Tread Area and Vertical Load

The tread area between the actual tire and the road surface may vary with steering and speed. The shape of the grounding area was assumed as an ellipse to simplify the load estimation algorithm for real-time processing. Measure the starting and end points of the strain gauge sensor output waveform as shown in Figure 10 to obtain an elliptical length L and measure the longitudinal length of the tire K and σ, and calculate the ground area with the road surface. The following equation (1) is to obtain the tire-slope tread area.

$$A = \pi \times \frac{L}{2} \times \frac{K}{2} \times \sigma \qquad (1)$$

Where, σ is the tread correction factor for considering the area where the tire does not touch the tire the road surface because of the tread. The horizontal length L of the ellipse can be obtained by measuring the strain gauge sensor.
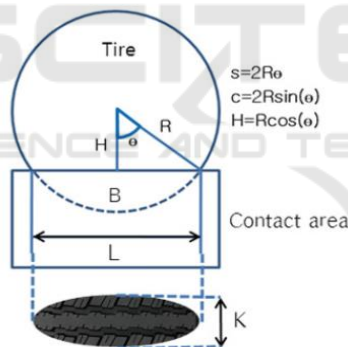

Figure 10: Tire contact patch.

The loads delivered to each tire using the section A obtained previously can be obtained in the following manner.

$$A = \frac{\alpha}{P} \qquad (2)$$
$$\alpha = -W \qquad (3)$$

Where α is the load, P is the air pressure, and W is the vertical drag. The load α is the opposite of the vertical force W.

4.2 Tire-road Longitudinal Contact Length

Figure 11 shows a data processing diagram using a strain gauge sensor signals. Figure 12 shows the output waveform of the strain gauge sensor attached to the tire. A secondary Butterworth filter was used to eliminate voltage noise from sensor signal in which the cut-off frequencies are 50 Hz and 1 Hz and a sampling frequency (f_s) is 5 kHz. Figure 13 shows the typical output waveform through the filter.
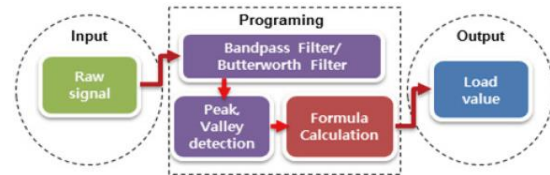

Figure 11: Data processing flow chart.

After going through the filter, the peak and the valley of the signal were found and the contact grounding time and speed were calculated. In the signal waveform shown in Figure 13, the two peaks of A and B are the points at which the tire deformation (contact with the road surface) begins and ends (Kim, Lee, Heo and Kim, 2014). Points C and D are the points at which the highest load is applied. Equation (4) is to obtain the ground contacting time(s), and equation (5) is to obtain the tire's rotational speed (v). The ground time was calculated by dividing the sampling frequency ($f_s = 5kHz$). The rotational speed was obtained using the difference in the number of samples at the peak points C and D and the circumference of the tire (T).
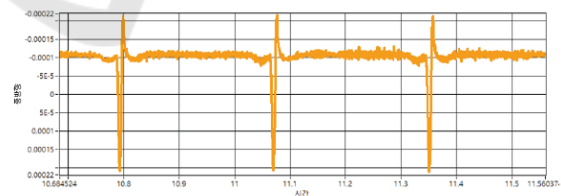

Figure 12: An example of strain gauge sensor signal.
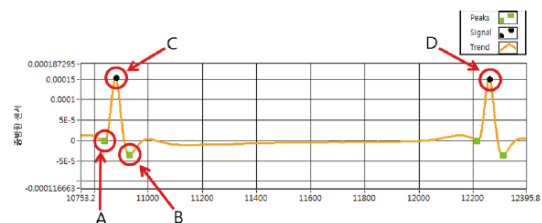

Figure 13: strain gauge sensor signal after the filter to longitudinal deformation of a tire.

$$s = \frac{B - A}{f_s} \quad (4)$$

$$v = \frac{f_s}{D - C} \times T \quad (5)$$

The lateral length of the tire contact surface L can be calculated using the tire's ground contacting time and the road surface's speed of rotation as follows.

$$L = v \times s \quad (6)$$

4.3 Tire-Road Lateral Contact Length

The tire-road lateral ground length K in equation (1) was experimentally extracted from the tread samples on the tires and on the road, as shown in Figure 14. As a result, the K-value is determined to vary depending on the tire air pressure, tire distortion and speed.

Figure 14: A sample of the K length under load.

The tire deformation corresponds to the y-axis value of the graph obtained through the strain gauge sensor as shown in Figure 15 below.
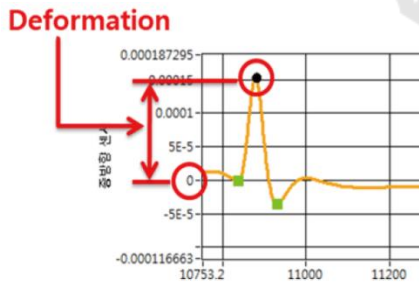

Figure 15: Longitudinal deformation data of a tire.

Table 2 shows the value of the sample K_i for the experimentally extracted lateral ground length for part of experimental results. The generalized relationship between K and tire pressures, deformation and vehicle speed, was found when tire pressures are 33, 35, and 37 (psi), loads are 285, 300, and 315 (kgf) and vehicle speeds are 25, 30 and 35 (kph) respectively to yield the equation (7). Where constants a~g were obtained by substituting 27 data

into the equation (8). The final results are shown in the equation (9), where x is the tire pressure (psi), y is the strain, and z is the vehicle speed (kph).

$$K = ax^2 + bx + cy^2 + dy \\ + ez^2 + fz + g \quad (7)$$

$$\begin{bmatrix} K_1 \\ K_2 \\ K_3 \\ \dots \\ K_{27} \end{bmatrix} = \begin{bmatrix} x_1^2 & x_1 & y_1^2 & y_1 & z_1^2 & z_1 & 1 \\ x_2^2 & x_2 & y_2^2 & y_2 & z_2^2 & z_2 & 1 \\ x_3^2 & x_3 & y_3^2 & y_3 & z_3^2 & z_3 & 1 \\ \dots & \dots & \dots & \dots & \dots & \dots & \dots \\ x_{27}^2 & x_{27} & y_{27}^2 & y_{27} & z_{27}^2 & z_{27} & 1 \end{bmatrix} \times \begin{bmatrix} a \\ b \\ c \\ d \\ e \\ f \\ g \end{bmatrix} \quad (8)$$

$$K = -0.073x^2 + 6.875x + 16.556y^2 \\ -60.416y + 0.0055z^2 - 0.94z - 62.817 \quad (9)$$

Table 2: The sample of the transverse K length between the tire and the road surface.

Tire Pressure (psi)	Average Deformation (10^4)	Calculated Velocity (km/h)	Measured K_i (cm)	Calculated K (cm)
33	1.10856	25.94	17.3	12.35
33	1.00524	31.13	16.6	13.2
33	0.89359	36.34	17.34	14.12
33	0.92663	25.96	21.97	11.9
35	1.18143	31.01	15.43	14.88
35	1.10675	36.21	15.18	16.4
35	1.25026	25.84	18.02	13.4
35	1.16392	31.05	17.55	14.58
37	1.32879	36.11	13.81	17.26
37	1.52354	25.81	17.95	13.68
37	1.33341	30.97	16.35	15.48
37	1.2957	30.99	17.45	15.48

4.4 Tire-Tread Correction Factor

Looking at the tread between the tire and the road surface in Figure 16, it can be seen that there are areas where the tread of the tire does not cause direct contact with the road surface. Therefore, the effect of the track should be considered in order to obtain an accurate ground area. The track correction factor is introduced to compensate for the change in the ground surface due to the track.

The tread correction factor was calculated experimentally using image pre-processing by printing the ground area between the tire and the road surface as shown in Figure 16 (Kang, Jung, Bae and Park, 1995). The tread correction factor, σ is the ratio between the non-contact empty area of a tire caused by the tread and the total elliptical contact area defined by the equation (10). actual

Figure 16: An example of tire-road contact area.

$$\sigma = \frac{\text{actual contact area}}{\text{total contact area}} \qquad (10)$$

Measured in the same 27 situations as measuring K length previously, the tracking correction factor was also found to vary with the pressure, strain and vehicle speed, as like in K length. Therefore, it was possible to obtain the calculation using Equation (11) in the same way as when the K-length was obtained. This is shown in Table 3.

$$\begin{aligned} K = &-0.00348x^2 - 0.301x \\ &-0.219y^2 + 0.819y - 0.000256z^2 \\ &+0.0183z + 5.904 \end{aligned} \qquad (11)$$

Table 3: Estimated results of tread correction factor.

Tire Pressure (psi)	Average Deformation (10^{-4})	Calculated Velocity (km/h)	Measured σ_i (cm)	Calculated σ (cm)
33	1.10856	25.94	0.686	0.704301
33	1.00524	31.13	0.675	0.686641
33	0.89359	36.34	0.673	0.646986
33	0.92663	25.96	0.628	0.636287
35	1.18143	31.01	0.601	0.618061
35	1.10675	36.21	0.597	0.600024
35	1.25026	25.84	0.629	0.618403
35	1.16392	31.05	0.632	0.612789
37	1.32879	36.11	0.579	0.56319
37	1.52354	25.81	0.597	0.575899
37	1.33341	30.97	0.568	0.558374
37	1.2957	30.99	0.542	0.549199

5 TEST RESULTS

Using the tread correction factor obtained in the previous section, and the lateral ground length K, longitudinal length L, the tire-road ground area A was obtained. The load was calculated using equation (2) and multiplied by 0.073 to express the tire pressure P by kgf. Table 4 shows the strain, estimated load from equation (2) and the error. As shown in the table, load estimates revealed very close to the experimental loads as a margin of error within 5%.

Table 4: Load error rate.

Tire Pressure (psi)	Average Deformation (10^{-4})	Calculated Velocity (km/h)	Calculated Load (kgf)	Error Rate (%)
33	1.10856	25.94	277.5748	2.605318
33	1.00524	31.13	280.1101	1.715765
33	0.89359	36.34	312.0626	4.020881
33	0.92663	25.96	310.9421	1.288208
35	1.18143	31.01	277.1663	2.748681
35	1.10675	36.21	298.5293	0.490228
35	1.25026	25.84	305.0755	1.691817
35	1.16392	31.05	324.8245	3.118884
37	1.32879	36.11	293.0514	2.82504
37	1.52354	25.81	311.2831	3.761046
37	1.33341	30.97	305.2585	1.752832
37	1.2957	30.99	310.8826	1.307118

6 CONCLUSIONS

In this paper, we proposed a method for measuring tire deformation through strain gauges and estimating the load applied to tires using them. Tire variations are closely related to the tread area between the tire and the road surface. To accurately calculate the ground area of a tire, a track correction factor was introduced and a correction factor value was derived experimentally. The contact time between the tire and the road surface was also calculated using a strain gauge sensor waveform. The results of the experiment showed that the difference between the estimated load value and the actual load was within 5%. The load estimation algorithm proposed in this study could be used to improve the chassis control system and to enhance the stability of automated driving of electrical vehicles

The next work is to perform more experiments with combination of diverse vertical loads, tire air pressures, and driving speeds to collect more information about the tire deformation. Based on these measured signal from stain gauge and diverse test conditions, a surrogate model or an artificial neural network could be constructed to further precisely descript the relation between tire load (vertical, longitudinal, and lateral directions) and measure signal. Finally, the tire contact force with the ground could be estimated based on the developed model.

REFERENCES

Ahn, B.-H., Bae, C.-H., Kim, H.-S., 2003. A study on the contact seam tracking sensor by using strain gauges, *The Journal of the Kore Institute of Maritime Information & Communication Sciences*, vol. 7, no. 5.

Kang, Y.-K., Jung, S.-W., Park, G.-T., 1995. Tire tread pattern classification using Fuzzy clustering algorithm, *Journal of Korean Institute of Intelligent Systems*. vol. 5, no. 2, pp. 44-57.

Kim, I.-H., Lee, J.-H., Heo, S.-J., Kim, J. G., 2014. A study of road friction coefficient estimation algorithm using intelligent tire system, *Autumn Conference and Exhibition of the Korean Society of Automotive Engineers*, pp. 321-326.

Matsuzaki, R, Todoroki, A., 2008. Wireless monitoring of automobile tires for intelligent tires, Sensors, vol. 8, no. 12., pp. 8123-8138.

Park, H., Gerdes, J. C., 2015. Optimal tire force allocation for trajectory tracking with an over-actuated vehicle, 2015 *IEEE Intelligent Vehicles Symposium*.